Hindawi
Mathematical Problems in Engineering
Volume 2022, Article ID 9080445, 13 pages
https://doi.org/10.1155/2022/9080445

Research Article

Finite-Time Convergence ESO-Based Nonsingular Fast Terminal Sliding Mode Control for PMSM with Unknown Parameters and Time-Varying Load

Chong-yi Gao,[1] Jun Dai,[1] Jing Li,[1] and Jian-xiong Li[2]

[1]*Key Lab of Intelligent Equipment Digital Design and Process Simulation of Hebei Province, Tangshan University, Tangshan 063000, China*
[2]*Key Lab of Industrial Computer Control Engineering of Hebei Province, Yanshan University, Qinhuangdao 066004, China*

Correspondence should be addressed to Jian-xiong Li; jxli@ysu.edu.cn

Received 7 October 2022; Revised 12 November 2022; Accepted 14 November 2022; Published 24 November 2022

Academic Editor: Xingling Shao

In this paper, an extended state observer (ESO)-based nonsingular fast terminal sliding mode (NFTSM) control method is proposed for the speed tracking system of permanent magnet synchronous motor (PMSM) in the present of unknown parameters and time-varying load. Firstly, three finite time convergence ESO (FTCESO) are employed to estimate the lumped disturbances in one speed loop and two current loops, respectively, and the estimates are fed forward to controllers for compensation. Secondly, a NFTSM controller is designed, which can drive the speed of PMSM track in desired speed in finite time. The stability of resulting closed-loop system is proved by using Lyapunov theory. Finally, the simulation and experimental results are compared with the existing methods, and the results show that the proposed method has better performance in tracking different kind of desired speed curves, and also performs better in reducing the chattering phenomenon.

1. Introduction

Due to the high-power density, high efficiency, and large torque-to-inertia ratio, permanent magnet synchronous motor (PMSM) has been widely used in various fields, such as robotics, aerospace actuators, and electric vehicles [1–3]. The field-orientation vector control is widely employed for high performance of PMSM, and it results a cascade control structure with an inner current control loop and an outer speed or torque control loop. It is well known that the PI control technique is still popular due to its simple implementation [4]. However, the PMSM system is nonlinear and strong coupling system with unavoidable uncertainties and parameter variations, as well as unknown load disturbances [2, 5]. In some cases, some parameters of PMSM are even unknown, for example, the stator resistance, inductance and flux linkage of motors of some old equipment are lost or changed considerably. In these cases, it would be difficult to achieve a high performance in the entire operating rage by only using linear control methods like PI control algorithm [6–8].

Aiming to achieve desired control performance, plenty of advanced control algorithms have been put forward for the PMSM drive system, such as adaptive control [1, 9], robust control [2], model predictive control [10, 11], sliding mode control (SMC) [7, 8], backstepping control [12], active disturbance rejection control (ADRC) [13, 14], disturbance observer-based control (DOBC) [2, 8, 15], and intelligent control [16–18]. These advanced control methods have improved the performance of the PMSM system from different aspects. Among these methods, the SMC has been considered as one of the most effective methods to deal with the uncertain nonlinear systems due to its insensitivity to uncertainties and disturbances [8, 19]. Terminal sliding mode control (TSMC) is a nonlinear SMC method and can achieve finite time stability [20]. The TSMC and its subsequent forms of improvement, nonsingular terminal sliding mode control (NTSMC), and nonsingular fast terminal

sliding mode control (NFTSMC) have been applied to control PMSMs as well to improve the dynamic performance and disturbance rejection, see [8, 19, 21] and therein.

However, the robustness of SMC or TSMC can only be guaranteed by the selection of large control gains, which will lead to the well-known chattering phenomenon. In particular, in some cases the exact upper bound of uncertainties or disturbances is difficult to obtain, so a particularly large control switching gain is naturally adopted to stabilize the system, but more serious chattering phenomenon will occur. For the case that the upper bound of the uncertainties of disturbances is unknown, the adaptive estimation technique has often been employed to estimate the upper bounds, and some adaptive SMC methods have been developed, such as [22–24].

A more effective strategy is to estimate and compensate the disturbances. In detail, the lumped disturbances are estimated by disturbance estimator and feed forward compensated in controller design [3, 25–27]. In [26], an aperiodic sampling based ESO was designed to estimate the disturbances for mobile robots with uncertainties, and then a robust antidisturbance kinetic control protocol was developed such that all error variables in the closed-loop system were bounded. In [27], a novel event-triggered unknown system dynamics estimator was designed to learn the uncertainties for quadrotors, and an adaptive event-triggered attitude control method with an appointed-time prescribed performance control was proposed. In [28], an unknown input observer was employed to estimate the unknown system dynamics of quadrotors. These works show that this strategy is available and effective. Moreover, under this strategy, it will be an alternative to use SMC for controller design. Since the lump disturbances are estimated and compensated, and a smaller gain will be selected to offset the estimation error instead of the disturbance in SMC, which will reduce the chattering phenomenon of SMC. In [8], a disturbance observer (DOB) was used to estimate the lumped disturbances, and a composite control method combing NTSMC with DOB, for short TSM + DOB method, was proposed for the speed loop of PMSM. In [29], a novel DOB was constructed based on the inverse model of the speed loop of PMSM to estimate the lumped disturbance, and the estimate value was introduced into the subsequent super-twisting sliding mode controller design. The current loops were governed still by two standard PI controllers in [8, 29]. In [30], the mismatched inductance of the PMSM was estimated by an ESO, and the estimate value was then introduced into a robust predictive controller for current control of PMSM. However, the load torque and other parameters of PMSM were considered to be certain and known. In [31], the speed and q-axis current were regulated in one loop, and a speed-current single-loop PMSM drive system was derived. A three-order ESO was designed to estimate the lumped disturbances for feedforward compensation, and a backstepping sliding mode controller was then proposed. Although TSMC method has been used in some of the literatures mentioned above, all of them cannot guarantee that the closed-loop system achieves finite time stability. Due to unknown load and parameter uncertainties, there is mismatched disturbances in PMSM, in which the mismatched disturbance means that the disturbance and the control input are not in the same channel. In [32], a finite time disturbance observer (FTDO) based NTSMC approach, short for "NTSMC-FTDO," was proposed for system with mismatched disturbance, and the PMSM was used as an example for experimental verification. Although the NTSMC-FTDO method solves the problem of mismatched disturbance, it could be found from the experimental results that there is still room for improvement in steady-state accuracy of speed tracking control of PMSM.

Based on the aforementioned analysis, this paper focuses on the finite-time control for speed tracking of PMSM in the presence of unknown parameters and uncertain parameters and time-varying load torque, and proposes a finite time convergence extend state observer (FTCESO) based NFTSM control method. Firstly, a finite time convergence extend state observer is employed to estimate the lumped disturbances including identification errors of some parameters, unknown load, and external disturbances. Secondly, the field-orientation vector control strategy is adopted, and a novel NFTSM control method is proposed to guarantee the closed loop system in finite time stability. The main contribution of this paper can be summarized as follows:

(1) The finite-time stability of the closed-loop system is guaranteed by using FTCESO-based NFTSM controller despite of mismatched uncertainties and disturbances. With the well estimation performance of the FTCESO for disturbances, the chattering phenomenon is weakened, and driven by the NFTSM controller, the high tracking performance of PMSM is achieved.

(2) The speed tracking control experiment is carried out on the PMSM experimental platform, in which some motor parameters are unknown. By comparing with the existing method, the experimental results show that the proposed method has better tracking accuracy while ensuring the transient performance.

The organization of this paper is as follows: in Section 2, the mathematical model of PMSM and the control problem formulation are given. The FTCESOs are designed to estimate the total disturbances in Section 3. Section 4 focuses on the NFTSM control design and its stability proof. In Section 5, the simulation and experimental results are presented, followed by conclusion in Section 6.

2. Problem Formulations and Preliminaries

Assume that magnetic circuit is unsaturated, hysteresis and eddy current loss are ignored, and the distribution of the magnetic field is sine space. In d-q coordinates, the model of surface mounted PMSM can be expressed as follows [8]:

$$\begin{cases} \dot{\omega} = \dfrac{3p_n\psi_f}{2J} i_q - \dfrac{B}{J}\omega + d_1, \\ \dot{i}_q = -\dfrac{R_s}{L_q} i_q - p_n \omega_{id} - \dfrac{p_n\psi_f}{L_q}\omega + \dfrac{1}{L_q} u_q + d_2, \\ \dot{i}_d = -\dfrac{R_s}{L_d} i_d + p_n \omega i_q + \dfrac{1}{L_d} u_d + d_3, \end{cases} \tag{1}$$

where ω is the speed of rotor, i_d and i_q are stator currents in d- and q- axis, respectively, u_d and u_q denote stator voltages in d- and q- axis, respectively, J is the moment of inertia, B is the viscosity friction coefficient, L_d and L_q are the stator d- and q- axis inductances, respectively, $L_d = L_q = L$, R_s is the stator resistance, p_n is the number of pole-paris, ψ_f is the magnetic flux linkage, and d_1, d_2, and d_3 denote the perturbations caused by parameter uncertainties and disturbances.

In some cases, due to a long time of application, some parameters would change greatly, or even be forgotten. In this paper, the values of J and B are considered to be uncertain and the parameters L, R_s, and ψ_f are regarded to be unknown. In addition, the load torque T_L is usually to be unknown. The unknown parameters could be identified offline. Let us put together the terms containing the uncertain and unknown parameters in the three channels of system (1), respectively, denoted by d_1, d_2, and d_3 as follows:

$$\begin{cases} d_1 = \dfrac{3p_n\left(J\Delta\psi_f - \psi_f\Delta J\right)}{2J(J+\Delta J)} i_q - \dfrac{J\Delta B - B\Delta J}{J(J+\Delta J)}\omega - \dfrac{T_L}{J+\Delta J}, \\ d_2 = \dfrac{R_s\Delta L - L\Delta R_s}{L(L+\Delta L)} i_q - \dfrac{L\Delta\psi_f - \psi_f\Delta L}{L(L+\Delta L)} p_n\omega - \dfrac{\Delta L}{L(L+\Delta L)} u_q, \\ d_3 = -\dfrac{L\Delta R_s - R_s\Delta L}{L(L+\Delta L)} i_d - \dfrac{\Delta L}{L(L+\Delta L)} u_d, \end{cases} \tag{2}$$

where ΔR_s, ΔL, and $\Delta\psi_f$ are identification errors of R_S, L, and ψ_f, respectively, and ΔJ and ΔB denote the errors between the real value and the nominal value of J and B, respectively.

In practice, these disturbances d_1, d_2, and d_3 are bounded due to physical limitations, and there first order time derivatives are also bounded. So, these disturbances satisfy the following assumption.

Assumption 1. The disturbance d_i is first order differentiable and assume that d_i and $\dot{d}_i$ are bounded, that is, there exist some positive constants $\overline{d}_i$ and $\overline{d}_{ti}$ such that $|d_i| \le \overline{d}_i$ and $|\dot{d}_i| \le \overline{d}_{ti}$, $i = 1, 2, 3$.

The main objective of this paper is to design controllers u_q and u_d so that the speed ω can track the desired speed ω_d in finite time in the presence of unknown parameters and time-varying load.

To end this section, a definition and three lemmas which will be used in finite time control and analysis later are as follows:

Lemma 1 (see [33]). *If there exists a Lyapunov function $V(x(t))$ such that the following inequality holds.*

$$\dot{V}(x(t)) + aV(x(t)) + bV^c(x(t)) \le 0, \forall t \ge t_0, \tag{3}$$

then the system state $x(t)$ will converge to the equilibrium in finite time, and the settling time t_1 can be given by the following equation:

$$t_1 \le t_0 + \frac{1}{a(1-c)} \ln \frac{aV^{1-c}(t_0) + b}{b}, \tag{4}$$

where $a > 0$, $b > 0$, $0 < c < 1$, and $t_0 \ge 0$ is the initial time.

Lemma 2 (see [34]). *For the following nonsingular fast terminal sliding mode, when the system state x reaches the sliding mode surface $s = 0$, the system state can converge to the origin in a finite time T_1.*

$$s = x + \lambda_1 sig^{\sigma_1}(x) + \lambda_2 \mathrm{sig}^{\sigma_2}(\dot{x}), \tag{5}$$

where $sig^{\sigma_i}(x) = sign(x)|x|^{\sigma_i}$, $sign(\cdot)$ is the sign function, $\lambda_1 > 0$, $\lambda_2 > 0$, $1 < \sigma_2 < 2$, and $\sigma_1 > \sigma_2$. The settling time T_1 is given by the following equation:

$$T_1 = \int_0^{|x(0)|} \frac{k_2^{1/\sigma_2}}{\left(x + k_1 x^{\sigma_1}\right)^{1/\sigma_2}} dx = \frac{\sigma_2 |x(0)|^{1-1/\sigma_2}}{k_1(\sigma_2 - 1)} \times F\left(\frac{1}{\sigma_2}; \frac{\sigma_2 - 1}{(\sigma_1 - 1)\sigma_2}; 1 + \frac{\sigma_2 - 1}{(\sigma_1 - 1)\sigma_2}; -k_1 |x(0)|^{\sigma_1 - 1}\right), \tag{6}$$

where $x(0)$ represents the initial value of x just after reaching the sliding surface and $F(\cdot)$ denotes Gauss' Hypergeometric function [35].

3. Finite-Time-Convergence Extended State Observers

In order to weaken the influence of the lumped disturbances on the control performance, three FTCESOs are used to estimate d_i and $i = 1, 2, 3$, respectively.

Let $x_{11} = \omega$, $x_{21} = i_q$, $x_{31} = i_d$, $x_{i2} = d_i$, and $i = 1, 2, 3$, then from equation (1), we have the following equation:

$$\begin{cases} \dot{x}_{i1} = a_i x_{i1} + g_i u_i + \psi_i + x_{i2} \\ \dot{x}_{i2} = \dot{d}_i \end{cases}, \quad i = 1, 2, 3, \tag{7}$$

where $a_1 = -B/J$, $a_2 = a_3 = -R_s/L$, $u_1 = 0$, $u_2 = u_q$, $u_3 = u_d$, $g_1 = 0$, $g_2 = g_3 = 1/L$, $\psi_1 = 3p_n\psi_f i_q/(2J)$, $\psi_2 = -p_n\omega i_d - p_n\psi_f\omega/L$, and $\psi_3 = p_n\omega i_q$.

The FTCESO can be designed for equation (7) as follows:

$$\begin{cases} \dot{\widetilde{x}}_{i1} = a_i\widehat{x}_{i1} + g_iu_i + \psi_i + \widehat{x}_{i2} - \eta_{i1}\mathrm{sign}\left(\widetilde{x}_{i1}\right) - \kappa_i\left(\mathrm{sig}^{\alpha_{i1}}\left(\widetilde{x}_{i1}\right)+\mathrm{sig}^{\beta_{i1}}\left(\widetilde{x}_{i1}\right)\right), \\ \dot{\widetilde{x}}_{i2} = -\kappa_i^2\left(\mathrm{sig}^{\alpha_{i2}}\left(\widetilde{x}_{i1}\right) + \mathrm{sig}^{\beta_{i2}}\left(\widetilde{x}_{i1}\right)\right) - \eta_{i2}\mathrm{sign}\left(\widetilde{x}_{i1}\right) \quad i = 1, 2, 3, \end{cases} \tag{8}$$

where $\widehat{x}_{ij}$ is the estimate of x_{ij}, $\widetilde{x}_{ij} = \widehat{x}_{ij} - x_{ij}$ denotes estimation error, $\kappa_i > 1$, $0.5 < \alpha_{i1} < 1$, $\alpha_{i2} = 2\alpha_{i1} - 1$, $\beta_{i1} = 1/\alpha_{i1}$, $\beta_{i2} = 1/\beta_{i1} + \beta_{i1} - 1$, $\eta_{ij} > 0$, $i = 1, 2, 3$, and $j = 1, 2$.

The estimate of disturbance d_i can be obtained as $\widehat{d}_i = \widehat{x}_{i2}$ and the estimation error is $\widetilde{d}_i = \widehat{d}_i - d_i$ and $i = 1, 2, 3$.

According to [36], if $\overline{d}_{ti}$ is known and $\eta_{i2} > \overline{d}_{ti}$ is chosen, then the estimation errors $\widetilde{x}_{i1}$ and $\widetilde{x}_{i2}$ will converge to zero in finite time, and the settling time is denoted as T_{oi}. Due to space limitations, the convergence analysis of the ESO (8) and the explicit expression of T_{oi} are omitted here. For detailed, please see [36].

Otherwise, $\overline{D_{Ti}}$ is unknown, following the analysis of [36], it is not difficult to deduce that the estimation errors $\widetilde{x}_{i1}$ and $\widetilde{x}_{i2}$ will converge to a neighborhood of the origin. The boundary of the neighborhood depends on $\overline{D_{Ti}}$ and η_{i2}, and a large η_{i2} will lead to a small boundary.

4. Nonsingular Fast Terminal Sliding Mode Controller Design

In field-oriented control strategy, the model of PMSM can be divided into three loops, one speed loop and two current loops. It can also be regarded as composed of two subsystems, a second-order subsystem consisting of speed loop and q-axis current loop and a first-order subsystem that is the d-axis current loop. The control structure diagram is shown in Figure 1.

For the second-order subsystem, the errors are defined as follows:

$$\begin{cases} e_1 = {}_{\omega d} - \omega \\ e_2 = \dot{\omega}_d - bi_q - a_1\omega - \widehat{d}_1 \end{cases}, \tag{9}$$

where $b = 3p_n\psi_f/2J$ and $\widehat{d}_1 = \widehat{x}_{12}$ obtained from equation (8).

From equations (1) and (9), one can get the following equation:

$$\begin{cases} \dot{e}_1 = e_2 + \widetilde{d}_1 \\ \dot{e}_2 = \ddot{\omega}_d - b\left(a_2i_q + g_2u_q + \psi_2 + d_2\right). \\ -a_1\left(\dot{\omega}_d - e_2 - \widetilde{d}_1\right) - \dot{\widetilde{d}}_1. \end{cases} \tag{10}$$

The nonsingular fast terminal sliding mode surface is chosen as follows:

$$s = e_1 + \lambda_1\mathrm{sig}^{\sigma_1}\left(e_1\right) + \lambda_2\mathrm{sig}^{\sigma_2}\left(e_2\right). \tag{11}$$

And the controller u_q is designed as follows:

$$u_q = u_{qeq} + u_{qn}, \tag{12}$$

$$\begin{aligned} u_{qeq} = \frac{L}{b}\Bigg(&\omega_d - a_1\dot{\omega}_d + a_1e_2 - \dot{\widehat{d}}_1 - a_2bi_q - b\psi_2 \\ &-b\widehat{d}_2 + \frac{1 + \lambda_1\sigma_1\left|e_1\right|^{\sigma_1 - 1}}{\lambda_2\sigma_2}\mathrm{sig}^{2-\sigma_2}\left(e_2\right)\Bigg), \end{aligned} \tag{13}$$

$$u_{qn} = \frac{L}{b}\left(k_1\mathrm{sign}\left(s\right) + k_2s\right), \tag{14}$$

where $\lambda_1 > 0$, $\lambda_2 > 0$, $1 < \sigma_2 < 2$, $\sigma_1 > \sigma_2$, $k_1 > 0$, and $k_2 > 0$.

It should be pointed out that d_1 is the mismatched disturbance which is not in the same channel as the control input u_q into the system. To eliminate the influence of mismatched disturbance on the system, the disturbance estimation $\widehat{d}_1$ is introduced into the sliding mode surface (11), which is inspired by [24]. If the estimation error $\widetilde{d}_1 = 0$, according to Lemma 2, when the error states of (10) reach into the surface $s = 0$, e_1 and e_2 could converge to zero in finite time.

Taking the time derivative of s and substituting (10) into it, one yields the following equation:

$$\begin{aligned} \dot{s} = &\left(1 + \lambda_1\sigma_1\left|e_1\right|^{\sigma_1 - 1}\right)\left(e_2 + \widetilde{d}_1\right) + \lambda_2\sigma_2\left|e_2\right|^{\sigma_2 - 1} \\ &\left(\ddot{\omega}_d - b \times \left(a_2i_q + g_2u_q + \psi_2 + d_2\right) - a_1\left(\dot{\omega}_d - e_2 - \widetilde{d}_1\right) - \dot{\widetilde{d}}_1\right). \end{aligned} \tag{15}$$

Substituting equations (12)–(14) into equation (15), one obtains the following equation:

$$\begin{aligned} \dot{s} = &\lambda_2\sigma_2\left|e_2\right|^{\sigma_2 - 1}\left(-k_1\mathrm{sign}\left(s\right) - k_2s + \left(a_1\widetilde{d}_1 + b\widetilde{d}_2\right)\right) \\ &+\left(1 + \lambda_1\sigma_1\left|e_1\right|^{\sigma_1 - 1}\right)\widetilde{d}_1. \end{aligned} \tag{16}$$

We first consider the case that the upper bound $\overline{d}_{ti}$ is known, the estimation error $\widetilde{d}_i = 0$ is achieved in finite time by using the FTCESOs (8), then the following main result is obtained.

Theorem 1. *For the error dynamics (10) with nonsingular fast terminal sliding mode surface (11), the controller (12)–(14) will drive the tracking error e_1 to converge to zero in finite time if the estimation errors of disturbances converge to zero in finite time.*

Proof. The proof will be divided into two steps, the first step is to prove that the system states do not escape in finite time, and the second step is to prove that the system states will converge to the origin in finite time.

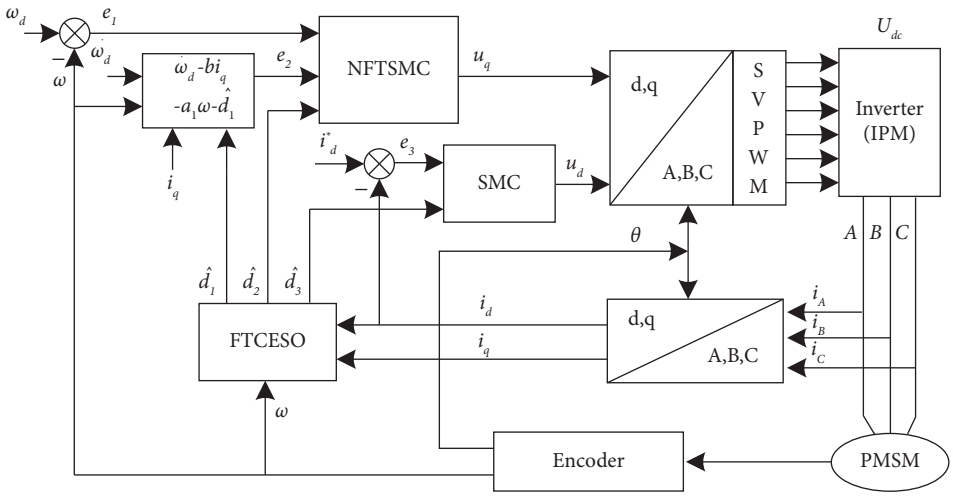

Figure 1: Structure of the FTCESO-based NFTSM control system.

(1) Following [24, 37], we define a finite time bounded function as $V_1 = 1/2(s^2 + e_1^2 + e_2^2)$. Taking the time derivative of V_1 along with equations (10) and (15), and substituting equations (12)–(16) into it, we can get the following equation:

$$\begin{aligned}\dot{V}_1 = {} & -\lambda_2\sigma_2|e_2|^{\sigma_2-1}\left(k_1|s| + k_2 s^2\right) + \lambda_2\sigma_2|e_2|^{\sigma_2-1}s\left(a_1\tilde{d}_1 + b\tilde{d}_2\right) \\ & + \left(1 + \lambda_1\sigma_1|e_1|^{\sigma_1-1}\right)s\tilde{d}_1 + e_1\left(e_2 + \tilde{d}_1\right) + e_2\left(a_1\tilde{d}_1 + b\tilde{d}_2\right) \\ & - k_1\mathrm{sign}(s) - k_2 s) - \frac{1 + \lambda_1\sigma_1|e_1|^{\sigma_1-1}}{\lambda_2\sigma_2}|e_2|^{3-\sigma_2}.\end{aligned} \tag{17}$$

Note that the inequality $|x|^\alpha < 1 + |x|$ holds for $x \in R$ and $0 < \alpha < 1$, then we have the following equation:

$$\begin{aligned}\dot{V}_1 \le {} & -k_1\lambda_2\sigma_2|e_2|^{\sigma_2-1}|s| - k_2\lambda_2\sigma_2|e_2|^{\sigma_2-1}s^2 + \lambda_2\sigma_2|e_2|^{\sigma_2-1} \\ & \times\left|b\tilde{d}_2 + a_1\tilde{d}_1\right||s| + \left|s\tilde{d}_1\right| + \lambda_1\sigma_1\left|s\tilde{d}_1\right||e_1|^{\sigma_1-1} + |e_1e_2| \\ & + \left|e_1\tilde{d}_1\right| + \left|e_2\tilde{d}_2\right| + k_1|e_2| + k_2|e_2 s| \\ & - \frac{1 + \lambda_1\sigma_1|e_1|^{\sigma_1-1}}{\lambda_2\sigma_2}|e_2|^{3-\sigma_2} \\ \le {} & \frac{1}{2}(3 + r_1 + r_2 + k_2)s^2 + \frac{1}{2}(2 + r_2)e_1^2 \\ & + \frac{1}{2}(3 + r_1 + k_2)e_2^2 + \frac{1}{2}\left(r_1^2 + r_2^2 + r_3^2 + k_1^2\right) + \left|\tilde{d}_1\right|^2 \\ \le {} & k_V V_1 + k_c,\end{aligned} \tag{18}$$

where $r_1 = \lambda_2\sigma_2|b\tilde{d}_2 + a_1\tilde{d}_1|$, $r_2 = \lambda_1\sigma_1|\tilde{d}_1|$, $r_3 = |\tilde{d}_2 + a_1/b\tilde{d}_1|$, $k_V = \max\{(3 + r_1 + r_2 + k_2), (2 + r_2), (3 + r_1 + k_2)\}$, and $k_c = \sup(1/2(r_1^2 + r_2^2 + r_3^2 + k_1^2) + |\tilde{d}_1|^2)$.

Since the estimation errors $\tilde{d}_1$ and $\tilde{d}_2$ are bounded, k_V and k_c are bounded constants, and it can be concluded from equation (18) that V_1, s, e_1, and e_2 will not escape in finite time [37].

(2) When the disturbance estimation error $\tilde{d}_1$ and $\tilde{d}_2$ converge to zero in a finite time, then equation (16) can be rewritten as follows:

$$\dot{s} = \lambda_2\sigma_2|e_2|^{\sigma_2-1}(-k_1\mathrm{sign}(s) - k_2 s). \tag{19}$$

Choose Lyapunov function candidate as $V_2 = 1/2s^2$, the time derivative of V_2 along with equation (19) is obtained as follows:

$$\dot{V}_2 = s\lambda_2\sigma_2|e_2|^{\sigma_2-1}(-k_1\mathrm{sign}(s) - k_2 s) \le -\varphi_1 V_2^{1/2} - \varphi_2 V_2, \tag{20}$$

where $\varphi_1 = \sqrt{2}k_1\lambda_2\sigma_2|e_2|^{\sigma_2-1}$ and $\varphi_2 = 2k_2\lambda_2\sigma_2|e_2|^{\sigma_2-1}$.

Since φ_1 and φ_2 contain error term e_2, phase trajectories are discussed in the following two cases. □

Case 1. When $e_2 \neq 0$, one has $\varphi_1 > 0$ and $\varphi_2 > 0$. According to Lemma 1, V_2 can converge to the sliding surface $s = 0$ within finite time T_3, and

$$T_3 \le \frac{2}{\varphi_1}\ln\frac{\varphi_1 {V_2}^{1/2}(t_0) + \varphi_2}{\varphi_2}, \tag{21}$$

where ${V_2}^{1/2}(t_0)$ is the initial value of the Lyapunov function V_2.

Case 2. When $e_2 = 0$, substituting the control law (12)–(14) into (10), yields the following equation:

$$\dot{e}_2 = -k_1\mathrm{sign}(s) - k_2 s, \tag{22}$$

which implies that $\dot{e}_2 < -k_1$ and $\dot{e}_2 > k_1$ for the case that $s > 0$ and $s < 0$, respectively. It can be seen that the system states will not always stay on the point ($e_2 = 0$ and $e_1 \neq 0$), so it is

reasonable to assume that there exists a small positive constant δ such that for a vicinity of $e_2 = 0$, i.e., $|e_2| \le \delta$ satisfies $\dot{e}_2 < -k_1$ and $\dot{e}_2 > k_1$ for $s > 0$ and $s < 0$, respectively. Thus, it yields that the crossing of trajectories between two boundaries of $|e_2| \le \delta$ is performed in finite time, and the dynamics from the region $|e_2| > \delta$ converge to the boundaries in finite time as well [20, 34]. Therefore, the sliding mode $s = 0$ can be reached from anywhere in the phase plane in finite time.

When the error states reach the sliding surface $s = 0$, equation (11) can be written as follows:

$$s = e_1 + \lambda_1 \mathrm{sig}^{\sigma_1}(e_1) + \lambda_2 \mathrm{sig}^{\sigma_2}(\dot{e}_1) = 0. \tag{23}$$

By Lemma 2, it can be concluded that e_1 can converge to the origin in finite time T_4, and T_4 is given as follows:

$$\begin{aligned} T_4 &= \int_0^{|e_1(0)|} \frac{{\lambda_2}^{1/\sigma_2}}{\left(e_1 + \lambda_1 {e_1}^{\sigma_1}\right)^{1/\sigma_1}} \mathrm{d}x \\ &= \frac{\sigma_2 |e_1(0)|^{1-1/\sigma_2}}{\lambda_1(\sigma_2 - 1)} F\left(\frac{1}{\sigma_2}; \vartheta; 1 + \vartheta; \lambda_1 |e_1(0)|^{\sigma_1 - 1}\right), \end{aligned} \tag{24}$$

where $\vartheta = \sigma_2 - 1/(\sigma_1 - 1)\sigma_2$ and $e_1(0)$ represents the initial value of the error state e_1 at the surface of the sliding mode $s = 0$. The proof is completed.

Theorem 1 establishes under the condition of $\tilde{d}_1 = 0$ and $\tilde{d}_2 = 0$. Next, we will discuss the case of $\tilde{d}_i \neq 0$ and $i = 1, 2$.

As mentioned above, when $\overline{d}_{t1}$ and $\overline{d}_{t2}$ (the boundaries of $\dot{d}_1$ and $\dot{d}_2$, respectively), are unknown, the FTCESOs (8) cannot guarantee that the estimation errors $\tilde{d}_1$ and $\tilde{d}_2$ converge to zero in finite time, but converge to the neighborhood of the origin. Rewriting equation (20) along with equation (16) yields the following equation:

$$\begin{aligned} \dot{V}_2 &= \lambda_2 \sigma_2 |e_2|^{\sigma_2 - 1} s\left(-k_1 \mathrm{sign}(s) - k_2 s + \left(a_1 \tilde{d}_1 + b\tilde{d}_2\right)\right) \\ &\quad + \left(1 + \lambda_1 \sigma_1 |e_1|^{\sigma_1 - 1}\right)\tilde{d}_1 s \\ &\le -\lambda_2 \sigma_2 |e_2|^{\sigma_2 - 1}\left(k_1 - \left|a_1 \tilde{d}_1 + b\tilde{d}_2\right|\right)|s| \\ &\quad - \lambda_2 \sigma_2 |e_2|^{\sigma_2 - 1} k_2 |s|^2 + \left(1 + \lambda_1 \sigma_1 |e_1|^{\sigma_1 - 1}\right)|\tilde{d}_1||s|. \end{aligned} \tag{25}$$

Since $|\tilde{d}_1|$ and $|\tilde{d}_2|$ will be very small by choosing large parameters η_{12} and η_{22} in FTCESOs (8), it is not difficult to select a large enough k_1 such that $k_1 - |a_1\tilde{d}_1 + b\tilde{d}_2| = \rho_1 \ge 0$.

Then, let $\rho_2 = \rho_1 \lambda_2 \sigma_2 |e_2|^{\sigma_2 - 1} - (1 + \lambda_1 \sigma_1 |e_1|^{\sigma_1 - 1})|\tilde{d}_1|$; following the above analysis, it is known that e_1 and e_2 will not escape in finite time, the point $e_2 = 0$ and $e_1 \neq 0$ is not a stable equilibrium, and e_2 will converge the boundaries of $|e_2| \le \delta$. It is reasonable to select a large enough k_1 such that $\rho_2 > 0$, then (25) would turn into $\dot{V}_2 \le -\varphi_2 V_2 - \sqrt{2\rho_2} V_2^{1/2}$ which implies Theorem 1 still holds.

In the case of $\rho_2 \le 0$, let $\rho_2' = -\rho_2 \ge 0$, one can obtain that,

$$\begin{aligned} \dot{V}_2 &\le -\lambda_2 \sigma_2 |e_2|^{\sigma_2 - 1} k_2 |s|^2 + \rho_2' |s| \\ &= -\left(\lambda_2 \sigma_2 |e_2|^{\sigma_2 - 1} k_2 |s| - \rho_2'\right)|s|, \\ |s| &\le \frac{\left(1 + \lambda_1 \sigma_1 |e_1|^{\sigma_1 - 1}\right)|\tilde{d}_1|}{k_2 \lambda_2 \sigma_2 |e_2|^{\sigma_2 - 1}} - \frac{k_1 - \left|a_1 \tilde{d}_1 + b\tilde{d}_2\right|}{k_2}. \end{aligned} \tag{26}$$

Therefore, bounded stability will be achieved, e_1 and e_2 will converge to converge to a neighborhood of the origin.

Remark 1. In order to reduce the chattering phenomenon, the signum function $\mathrm{sign}(\cdot)$ used in (14) could be replaced by a continuous function, such as hyperbolic tangent function $\tanh(k_{th}x) = e^{k_{th}x} - e^{-k_{th}x}/e^{k_{th}x} + e^{-k_{th}x}$, and for any $k_{th} > 0$ and $x \in \mathfrak{R}$, the following inequality holds [38].

$$0 \le x\left(\mathrm{sign}(x) - \tanh\left(k_{th}x\right)\right) \le \frac{\delta}{k_{th}}, \tag{27}$$

where δ is a constant that satisfies $\delta = e^{-(\delta+1)}$ and $\delta = 0.2785$. Therefore, if a large parameter k_{th} is chosen, the hyperbolic tangent function is approximately equivalent to the signum function.

At last, let $e_3 = i_d^* - i_d = -i_d$, the d-axis current loop can be rewritten as follows:

$$\dot{e}_3 = -a_3 e_3 - \psi_3 - g_{3\,ud} - d_3. \tag{28}$$

The controller u_d is designed as follows

$$_{ud} = L\left(-a_3 e_3 - \psi_3 - \hat{d}_3 + k_3 sign(e_3) + k_4 e_3\right), \tag{29}$$

where $k_3 > 0$ and $k_4 \ge 0$.

Choosing Lyapunov function $V_3 = 1/2e_3^2$, taking its time derivative along with equation (28) and substituting equation (29) into it, it follows.

$$\begin{aligned} \dot{V}_3 &= e_3\left(-k_3 \mathrm{sign}(e_3) - k_4 e_3 - \tilde{d}_3\right) \\ &\le -k_4 e_3^2 - \left(k_3 - |\tilde{d}_3|\right)|e_3| \\ &= -2k_4 V_3 - \sqrt{2}\left(k_3 - |\tilde{d}_3|\right)V_3^{1/2}. \end{aligned} \tag{30}$$

Since $|\tilde{d}_3|$ is bounded, and it will be small by choosing appropriate parameter η_{32}. Therefore, it is not difficult to choose a large enough k_3 such that $k_3 - |\tilde{d}_3| > 0$. Then, it can be concluded that e_3 will converge to zero in finite time by using Lemma 2.

5. Simulation and Experimental Results

In order to illustrate the effectiveness and practicability of the proposed method, the proposed method and NTSMC-FTDO method proposed in [32] are carried out in simulation and experiment.

5.1. PMSM Parameters Identification. In the experimental platform, some parameters of the PMSM are unknown, such as R_s, L, and ψ_f. These parameters are identified by offline methods.

5.1.1. Identification of R_s. The stator windings of the motor in the experiment are star connection. The stator resistance R_s is estimated by an offline experiment. Short-circuit the motor phase B and phase C terminals together, and apply a DC voltage u_d between A and B terminals, the stator resistance R_s could be estimated by the following relational expression.

$$R_s = \frac{2}{3}\frac{u_d}{i_d}, \tag{31}$$

where i_d is the current stable value of the closed loop circuit.

5.1.2. Identification of L. Since $L_d = L_q = L$ in surface PMSM, we just identify one of them.

The motor stator is stationary and the d-axis current changes over time until it reaches saturation. It could be found that the rise of the current from zero to steady value is exponential, so we can calculate the d-axis inductor L_d by taking the time for the current to rise. Specifically, recording the time when the current rises from zero to 0.632 times of steady value, that is, $t_{0.632}$, then we can get the following equation:

$$L_d = t_{0.632}R_s. \tag{32}$$

5.1.3. Identification of ψ_f. The magnetic flux linkage of rotor is essentially equal to the back electromotive force (EMF) coefficient, but in different units. The relationship between them is as follows:

$$K_e = p\psi_f 1000\frac{2\pi}{60}, \tag{33}$$

where K_e is the back EMF coefficient, and it could be obtained by the following empirical formula in engineering.

$$K_e = K\frac{P_N p}{f_N I_N}, \tag{34}$$

where P_N, f_N, and I_N are the rated power, rated frequency, and rated current of the motor, respectively. K is the correction factor which is taken as $K = 9.62$ in engineering.

The parameters of the motor are shown in Table 1.

5.2. Simulation Results. The two comparison methods and their design parameters are as follows:

(1) The proposed method (NFTSMC-FTCESO).

FTCESOs: $\kappa_1 = \kappa_2 = \kappa_3 = 4000$, $\eta_{11} = \eta_{21} = \eta_{31} = 200$, $\eta_{12} = \eta_{22} = \eta_{32} = 10$, and $\alpha_{11} = \alpha_{21} = \alpha_{31} = 0.6$.

NFTSMC: $\lambda_1 = 0.5$, $\lambda_2 = 0.001$, $\sigma_1 = 7/5$, $\sigma_2 = 9/7$, $k_1 = 1$, $k_2 = 20$, $k_3 = 10$, $k_4 = 0.1$, and $k_{th} = 20$.

(2) NTSMC-FTDO [30].

In this method, the controller is designed as follows:

$$u_{q2} = -\frac{L}{b}\Bigg(-\beta\frac{q}{p}e_2^{2q-p/q} - \ddot{\omega}_d + b\left(a_1 i_q + \psi_2 + \hat{d}_2\right) + a_1\dot{\omega} + \dot{\hat{d}}_1 - k_1'\mathrm{sig}^{\sigma_3}(s) - k_2' s\Bigg). \tag{35}$$

And u_d controller is the same as in this paper. The parameters are chosen as: $n_0 = 20$, $n_1 = 50$, $n_2 = 15$, $H_1 = 2 \times 10^4$, $H_2 = H_3 = 1 \times 10^4$, $\beta = 1000$, $p/q = 9/7$, $k_1' = 1$, $k_2' = 20$, and $\sigma_3 = 0.9$.

In the simulation, the following time-varying load is considered $T_L = \begin{cases} 1 + 0.2\sin(2\pi t), t \le 0.3\text{s} \\ 2 + 0.2\sin(2\pi t), t > 0.3\text{s} \end{cases}$

Figures 2 and 3 show that the motor tracks a step reference signal and a time-varying signal, respectively, where the step reference speed n_d is changed from 300 to 800 r/min at 0.5 s, and the time-varying signal is as follows: $nd = 60/2\pi\ \omega d = 500 + 50\sin(\pi t)$ r/min.

It could be found from Figures 1 and 3 that both control methods can track the reference signals well in the presence of uncertain parameters and unknown time-varying load. In contrast, the proposed control method performs better in terms of the disturbance rejection, tracking accuracy, and dynamic adjustment in case of sudden change in reference signal or load, see Figures 2(a) and 3(a), the tracking error is within 2 r/min under the proposed method, but 4 r/min or more under the NTSMC-FTDO method.

In addition, by analyzing the two algorithms, it could be concluded that the influence of the estimation of the mismatched disturbance on the tracking performance is far greater than that of the estimation of the matched disturbances. Specifically, in the proposed method, $\hat{d}_1$ is introduced into the sliding mode surface to eliminate the mismatched disturbance d_1. While $\hat{d}_2$ and $\hat{d}_3$ are introduced into the controllers u_q and u_d for feedforward compensation the matched disturbances d_2 and d_3, respectively. Obviously, the estimation errors $\tilde{d}_2$ and $\tilde{d}_3$ could be offset by the two switching terms $k_1 sign(s)$ and $k_3 sign(e_3)$, respectively, but eliminating the influence of d_1 on tracking error could only depend on the accuracy of the disturbance observer. Therefore, the curves of $\hat{d}_1$ are given in the simulation results, as well as in the following experimental results. As can be seen from Figures 2(b) and 3(b), both two methods have little difference in the estimation effect of d_1 in the simulation, and the results of the proposed method are relatively smooth.

5.3. Experimental Results. The experimental platform is shown in Figure 4, where DS1104 control card of dSPACE is used as the controller, and CP1104 is the interface between DS1104 and relevant devices such as power module, encoder, and load drive unit. In the power module, PS21265-AP IPM made by Mitsubishi Electric Corporation is used. The load torque is supplied by a magnetic powder brake, and the torque is proportional to the reference signal voltage

Table 1: The parameters of PMSM.

Parameters	Known/nominal value	Unknown	
		Used in simulation model	Identified
Rated power (P/W)	180		
Rated voltage (V)	380		
Pole-pairs (p)	2		
Rated speed (n/(r/min))	1500		
Inertia coefficient (J/kg·m^2)	0.0008	0.0009	
Viscosity coefficient (B)	0.0025	0.002	
Stator resistance (R_s/Ω)		12.4	12.5
Inductance (L/H)		0.18	0.1875
Flux linkage (ψ_f/Wb)		0.95	0.945

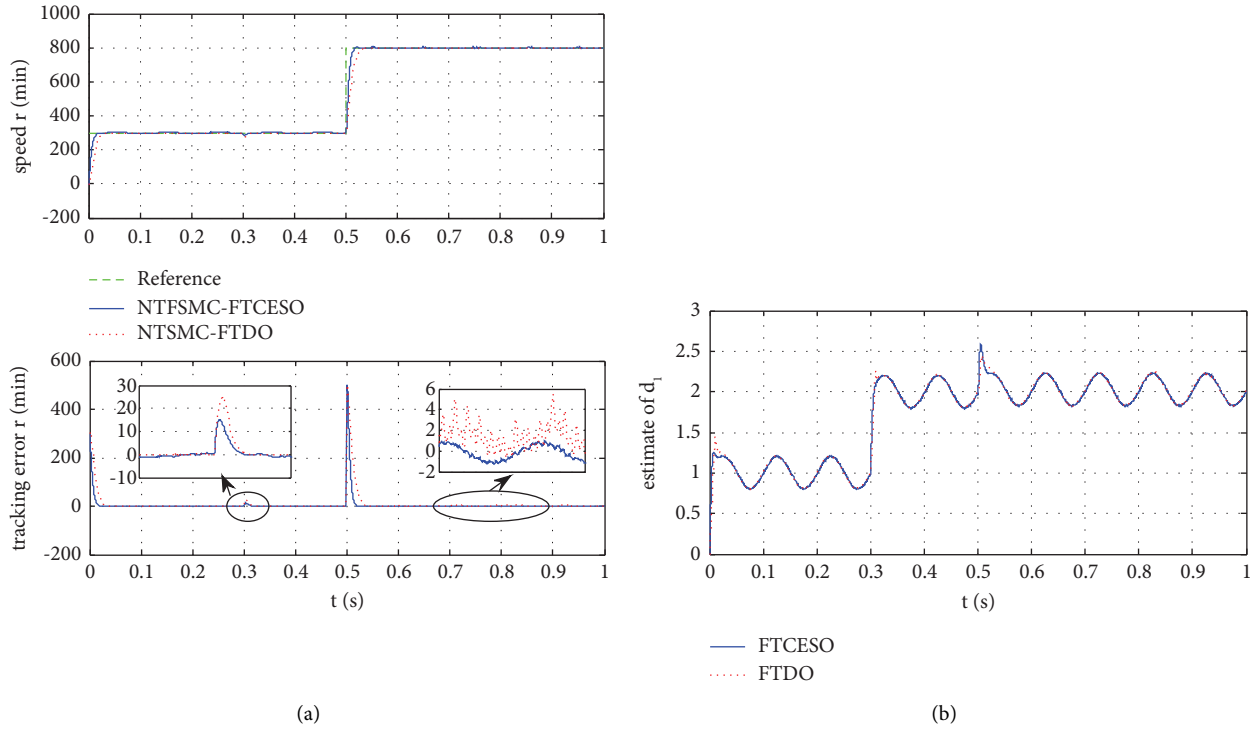

Figure 2: Simulation results of step signal tracking. (a) Speed and tracking error. (b) Estimate of d_1.

generated by the DS1104 and driven by a load drive unit to drive the magnetic powder brake.

The experiment is carried out in the following four cases:

Case 1: Tracking the reference signal 1 under load 1

Case 2: Tracking the reference signal 1 under load 2

Case 3: Tracking the reference signal 2 under load 1

Case 4: Tracking the reference signal 2 under load 2

Where the reference signals and loads are as follows:
Reference signal 1 (step signal):

$$n_d = \frac{60}{2\pi}\omega_d = \begin{cases} 100\,\text{r/min} & t < 5\,\text{s} \\ 500\,\text{r/min} & t \geq 5\,\text{s} \end{cases}. \tag{36}$$

Reference signal 2 (time-varying signal):

$$n_d = \frac{60}{2\pi}\omega_d = 500 + 50\sin(\pi t)\text{r/min}, \tag{37}$$

Load 1 (abrupt changing load):

$$T_L = \begin{cases} 0.3\,\text{N}\cdot\text{m}, t \leq 5\text{s} \\ 1.04\,\text{N}\cdot\text{m}, t > 5\text{s} \end{cases}. \tag{38}$$

Load 2 (time-varying load):

$$T_L = 0.5 + 0.2\sin(\pi t)\text{N}\cdot\text{m}. \tag{39}$$

Same as simulation, the two methods, the proposed control method, and the NTSMC-FTDO method [32] are tested on the experimental platform and the experimental results are shown in Figures 5–8, in which the subfigures (a) show the speed tracking and tracking errors and subfigures (b) present the estimations of mismatched disturbance d_1 in the four cases, respectively.

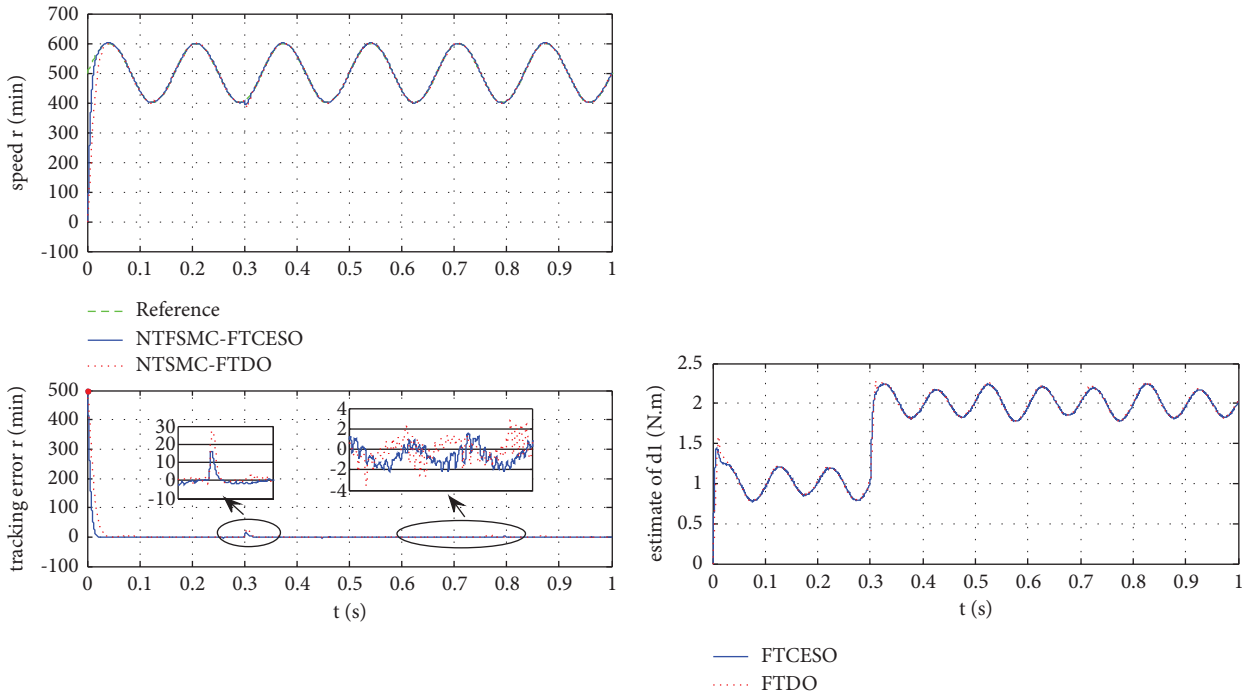

Figure 3: Simulation results of time-varying signal tracking. (a) Speed and tracking error. (b) Estimate of d_1.

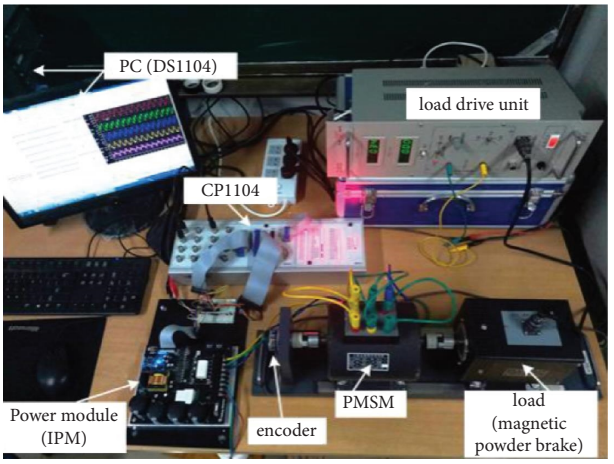

Figure 4: PMSM experimental platform.

It can be found that the proposed method has better performance on speed tracking and disturbance rejection than that of the NTSMC-FTDO method in all the four cases, see the speed tracking in subfigure (a) of Figures 5–8. In detail, from Figure 5(a), the speed tracking error is within 15 r/min under the proposed method while 40 r/min under the NTSMC-FTDO method of [32] in case 1. And the proposed method also has better transient performance than that of NTSMC-FTDO method. In case 2, when the load is time-varying, the tracking error under the proposed method is within 10 r/min, while 20 r/min under the NTSMC-FTDO method at lower speed, see Figure 6(a). When the speed goes up to 500 r/min, the tracking errors of both methods increase, but the performance of the proposed method is relatively better, see Figure 5(a). When the reference is a time-varying signal, the comparison of the two methods is similar to the case of step signal, see Figure 6(a).

Moreover, it could be found that the tracking performance of the proposed method in tracking time-varying signal is better than that in tracking step signal, but the NTSMC-FTDO method is different, see Figures 7(a) and 8(a). A potential reason is that the estimation of the lumped disturbance d_1

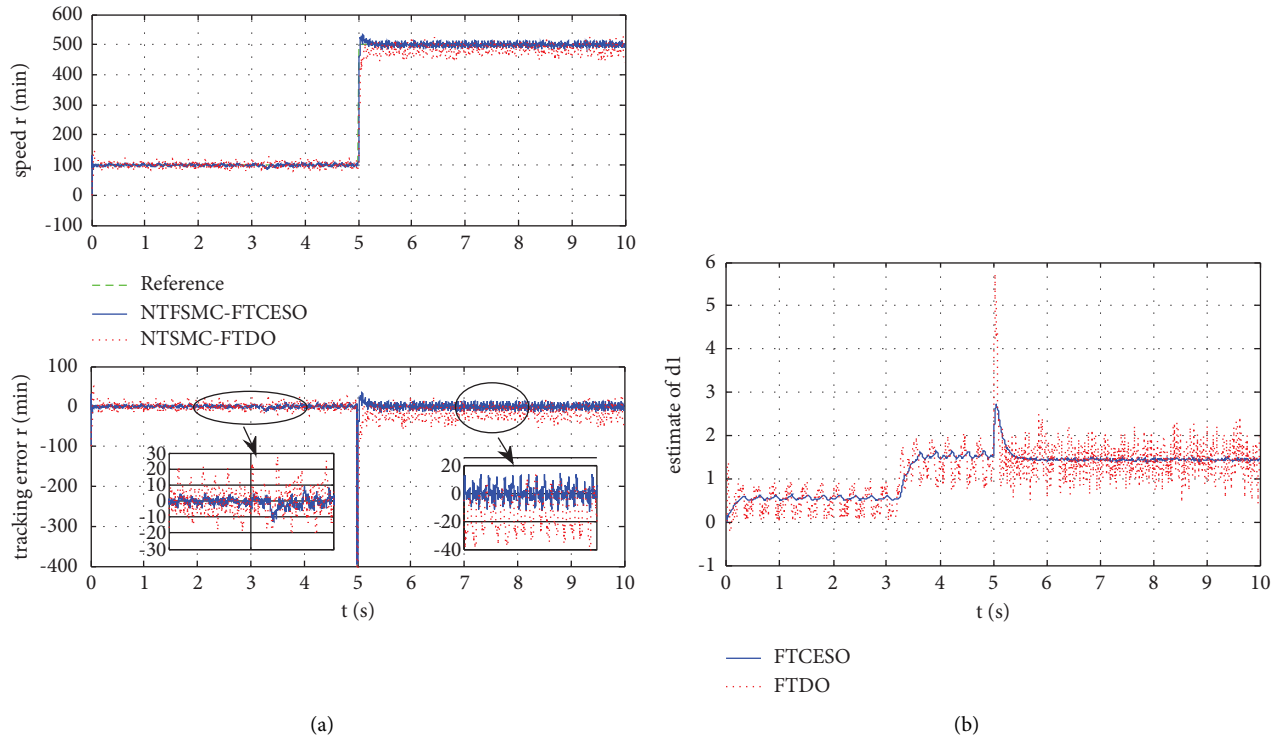

FIGURE 5: Experimental results of step signal tracking under abrupt changing load (case 1). (a) Speed and tracking error. (b) Estimate of d_1.

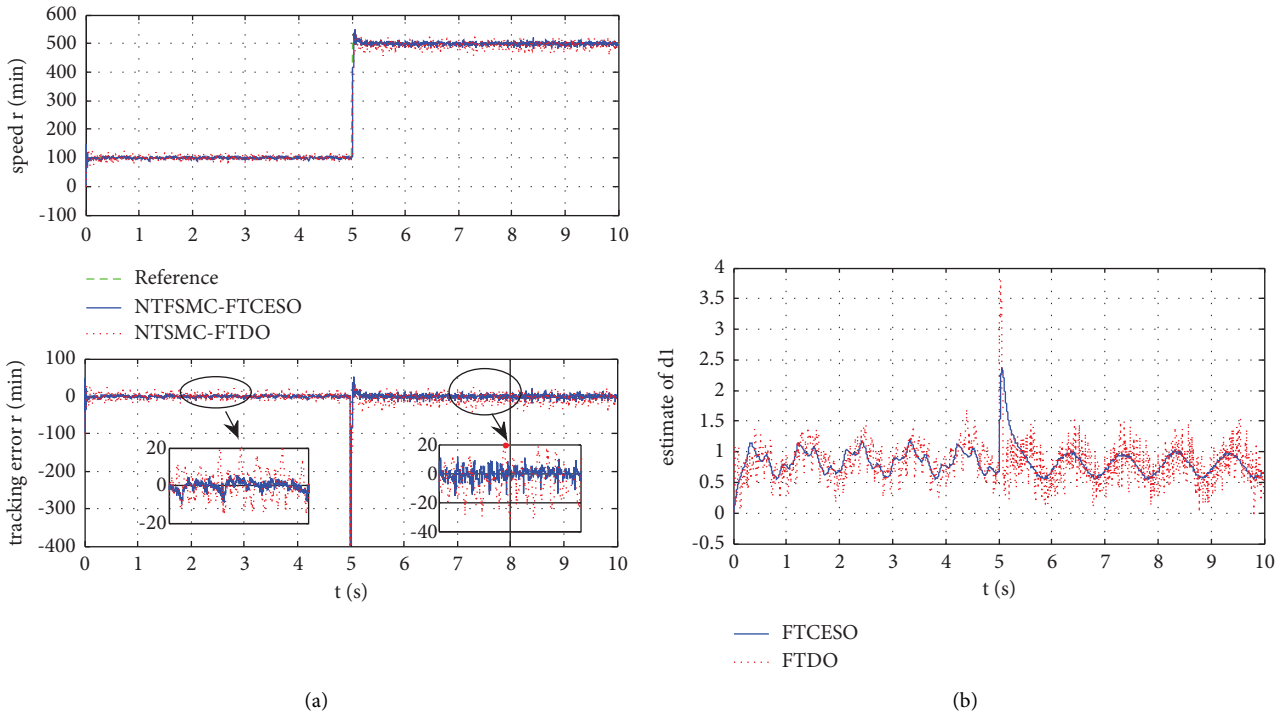

FIGURE 6: Experimental results of step abrupt signal tracking under time-varying load (case 2). (a) Speed and tracking error. (b) Estimate of d_1.

could affect the tracking error. The estimation accuracy of the FTCESO employed in the proposed method is better than that of the other, see Figures 7(b) and 8(b). In fact, the performance of disturbance estimation and tracking are mutually influenced, since the tracking performance also affects the disturbance estimation through the estimate of the states.

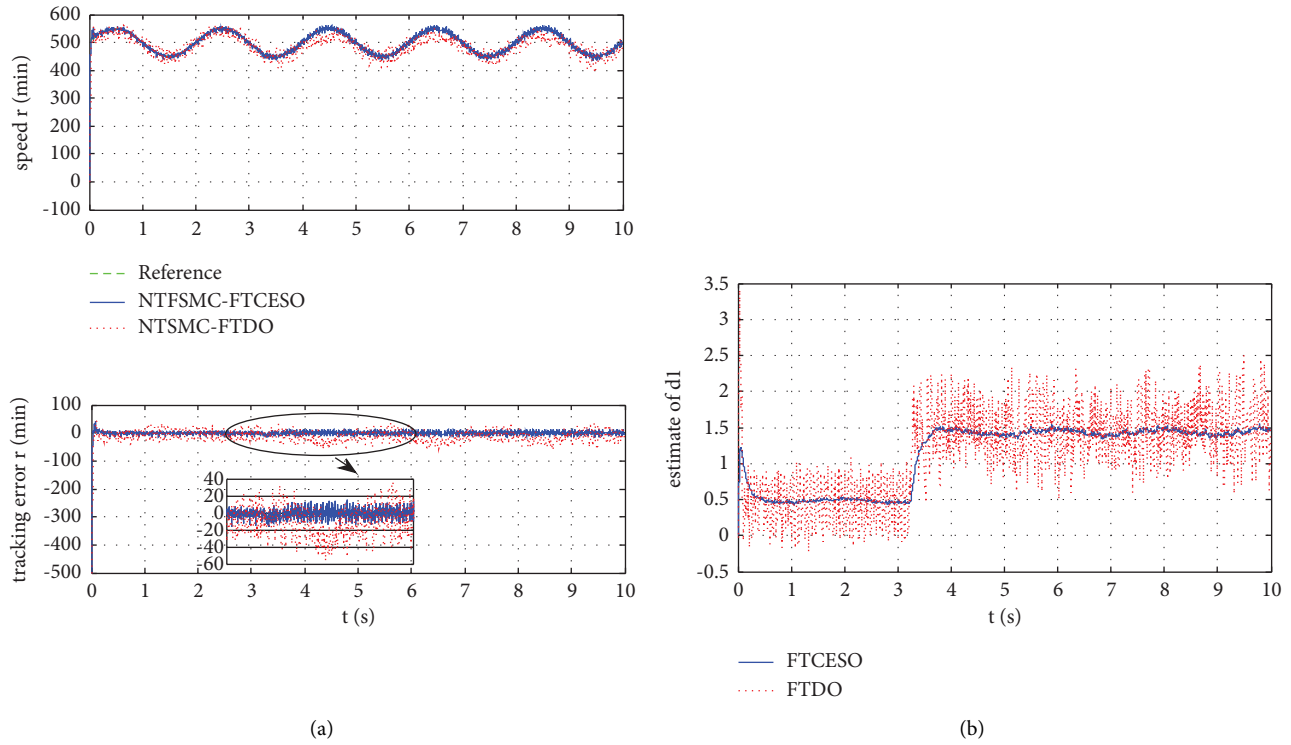

Figure 7: Experimental results of time-varying signal tracking under abrupt changing load (case 3). (a) Speed and tracking error. (b) Estimate of d_1.

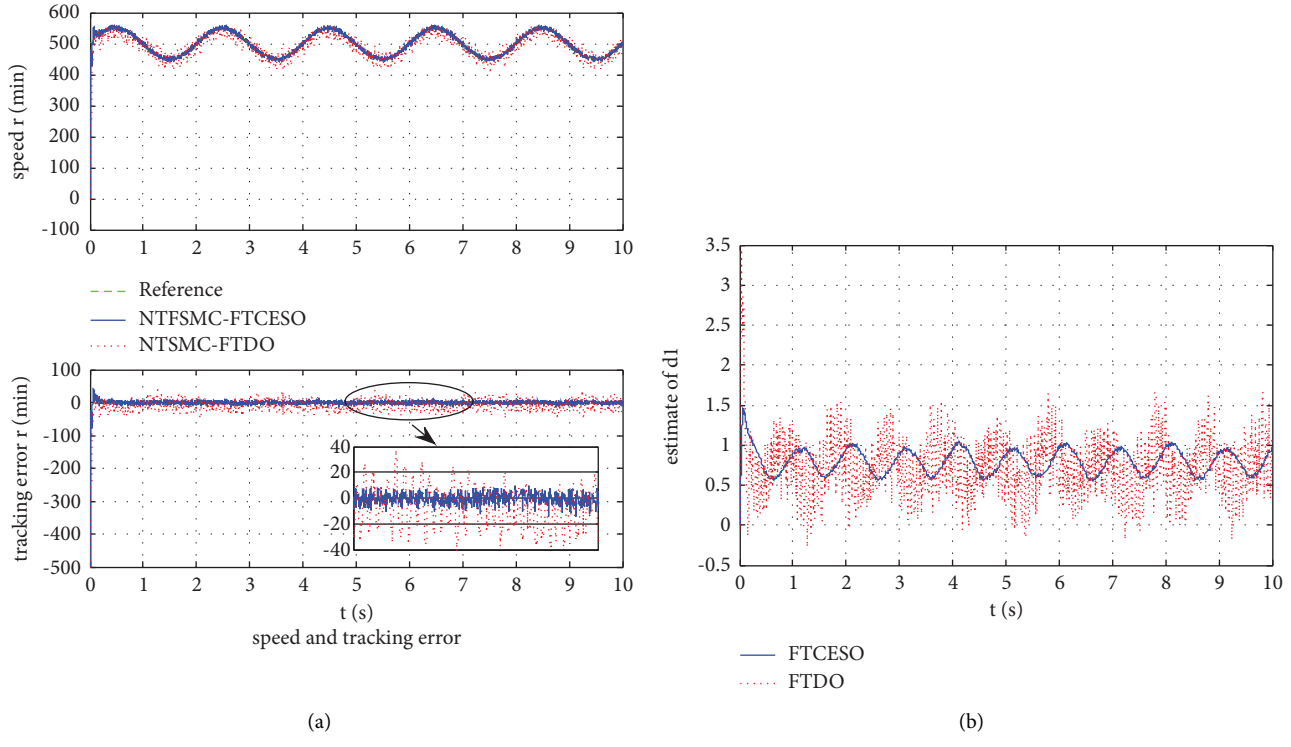

Figure 8: Experimental results of time-varying signal tracking under time-varying load (case 4). (a) Speed and tracking error. (b) Estimate of d_1.

6. Conclusion

The speed tracking problem of PMSM with unknown parameters and time-varying load is investigated in this paper, and a FTCESO-based-NFTSMC method is proposed to improve the tracking performance of the PMSM against the matched and mismatched uncertainties and disturbances. The lumped disturbances are well estimated by using FTCESOs and then compensated by feedforward. Finite time stability could be achieved when the upper bounds of the derivatives of the lumped disturbances are known, and the speed tracking error could converge to a neighborhood of the zero in finite time when the bounds are unknown. Finally, simulation and experiment are carried out to illustrate the effectiveness of the proposed method, and the simulation and experimental results show that the proposed method has high tracking accuracy, fast convergence speed, and strong robustness.

Data Availability

The data used to support the findings of this study are included within the article.

Conflicts of Interest

The authors declare that there are no conflicts of interest regarding the publication of this paper.

Acknowledgments

This work was supported in part by the Science and Technology Project of Hebei Education Department under Grants nos. ZD2021102 and BJ2019209, in part by the Science and Technology Innovation Team Training Project of Tangshan under Grant no. 21130205D, in part by the Tangshan Talent Funding Project under Grant no. A202203031, and in part by the Provincial Key Laboratory Performance Subsidy Project under Grant no. 22567612H.

References

[1] S. Li and Z. Liu, "Adaptive speed control for permanent-magnet synchronous motor system with variations of load inertia," *IEEE Transactions on Industrial Electronics*, vol. 56, no. 8, pp. 3050–3059, 2009.

[2] Y. A.-R. I. Mohamed, "Design and implementation of a robust current control scheme for a PMSM vector drive with a simple adaptive disturbance observer," *IEEE Transactions on Industrial Electronics*, vol. 54, no. 4, pp. 1981–1988, 2007.

[3] J. Yang, W. H. Chen, S. H. Li, L. Guo, and Y. Yan, "Disturbance/uncertainty estimation and attenuation techniques in PMSM drives—a survey," *IEEE Transactions on Industrial Electronics*, vol. 64, no. 4, pp. 3273–3285, 2017.

[4] G. J. Wang, C. T. Fong, and K. J. Chang, "Neural- network-based self-tuning PI controller for precise motion control of PMAC motors," *IEEE Transactions on Industrial Electronics*, vol. 48, no. 2, pp. 408–415, 2001.

[5] Y. Feng, X. H. Yu, and F. L. Han, "High-order terminal sliding-mode observer for parameter estimation of a permanent-magnet synchronous motor," *IEEE Transactions on Industrial Electronics*, vol. 60, no. 10, pp. 4272–4280, 2013.

[6] K. H. Kim and M. J. Youn, "A nonlinear speed control for a PM synchronous motor using a simple disturbance estimation technique," *IEEE Transactions on Industrial Electronics*, vol. 49, no. 3, pp. 524–535, 2002.

[7] X. Zhang, L. Sun, K. Zhao, and L. Sun, "Nonlinear speed control for PMSM system using sliding-mode control and disturbance compensation techniques," *IEEE Transactions on Power Electronics*, vol. 28, no. 3, pp. 1358–1365, 2013.

[8] S. H. Li, M. Zhou, and X. H. Yu, "Design and implementation of terminal sliding mode control method for PMSM speed regulation system," *IEEE Transactions on Industrial Informatics*, vol. 9, no. 4, pp. 1879–1891, 2013.

[9] H. H. Choi, N. T. T. Vu, and J. W. Jung, "Digital implementation of an adaptive speed regulator for a PMSM," *IEEE Transactions on Power Electronics*, vol. 26, no. 1, pp. 3–8, 2011.

[10] S. X. Niu, Y. X. Luo, W. N. Fu, and X. D. Zhang, "Robust model predictive control for a three-phase PMSM motor with improved control precision," *IEEE Transactions on Industrial Electronics*, vol. 68, no. 1, pp. 838–849, 2021.

[11] K. Belda and D. Vošmik, "Explicit generalized predictive control of speed and position of PMSM drives," *IEEE Transactions on Industrial Electronics*, vol. 63, no. 6, pp. 3889–3896, 2016.

[12] M. Morawiec, "The adaptive backstepping control of permanent magnet synchronous motor supplied by current source inverter," *IEEE Transactions on Industrial Informatics*, vol. 9, no. 2, pp. 1047–1055, 2013.

[13] H. Sira-Ramirez, J. Linares-Flores, C. Garcia-Rodriguez, and M. A. Contreras-Ordaz, "On the control of the permanent magnet synchronous motor: an active disturbance rejection control approach," *IEEE Transactions on Control Systems Technology*, vol. 22, no. 5, pp. 2056–2063, 2014.

[14] G. Zhang, G. Wang, B. Yuan, R. Liu, and D. Xu, "Active disturbance rejection control strategy for signal injection-based sensorless IPMSM drives," *IEEE Trans. Transp. Electr.*vol. 4, no. 1, pp. 330–339, 2018.

[15] E. Sariyildiz and K. Ohnishi, "Stability and robustness of disturbance observer-based motion control systems," *IEEE Transactions on Industrial Electronics*, vol. 62, no. 1, pp. 414–422, 2015.

[16] V. Q. Leu, H. H. Choi, and J. W. Jung, "Fuzzy sliding mode speed controller for PM synchronous motors with a load torque observer," *IEEE Transactions on Power Electronics*, vol. 27, no. 3, pp. 1530–1539, 2012.

[17] F. J. Lin, Y. C. Hung, and K. C. Ruan, "An intelligent second-order sliding-mode control for an electric power steering system using a wavelet fuzzy neural network," *IEEE Transactions on Fuzzy Systems*, vol. 22, no. 6, pp. 1598–1611, 2014.

[18] S. Li, H. Won, X. Fu, M. Fairbank, D. C. Wunsch, and E. Alonso, "Neural-network vector controller for permanent-magnet synchronous motor drives: simulated and hardware-validated results," *IEEE Transactions on Cybernetics*, vol. 50, no. 7, pp. 3218–3230, 2020.

[19] J. Zheng, H. Wang, Z. Man, J. Jin, and M. Fu, "Robust motion control of a linear motor positioner using fast nonsingular terminal sliding mode," *IEEE*, vol. 20, no. 4, pp. 1743–1752, 2015.

[20] Y. Feng, X. H. Yu, and Z. H. Man, "Non-singular terminal sliding mode control of rigid manipulators," *Automatica*, vol. 38, no. 12, pp. 2159–2167, 2002.

[21] W. Xu, A. K. Junejo, Y. Liu, and M. R. Islam, "Improved continuous fast terminal sliding mode control with extended

state observer for speed regulation of PMSM drive system," *IEEE Transactions on Vehicular Technology*, vol. 68, no. 11, pp. 10465–10476, 2019.

[22] Y. J. Huang, T. C. Kuo, and S. H. Chang, "Adaptive sliding-mode control for nonlinear systems with uncertain parameters," *IEEE Transactions on Systems, Man, and Cybernetics, Part B (Cybernetics)*, vol. 38, no. 2, pp. 534–539, 2008.

[23] C. Fang, C. Huang, and S. Lin, "Adaptive sliding-mode torque control of a PM synchronous motor," *IEE Proceedings - Electric Power Applications*, vol. 149, no. 3, pp. 228–236, 2002.

[24] L. Qiao and W. D. Zhang, "Adaptive non-singular integral terminal sliding mode tracking control for autonomous underwater vehicles," *IET Control Theory & Applications*, vol. 11, no. 8, pp. 1293–1306, 2017.

[25] J. Zhang, X. Shao, W. Zhang, and J. Na, "Path-following control capable of reinforcing transient performances for networked mobile robots over a single curve," *IEEE Transactions on Instrumentation and Measurement*, p. 1, 2022.

[26] X. Shao, J. Zhang, and W. Zhang, "Distributed cooperative surrounding control for mobile robots with uncertainties and aperiodic sampling," *IEEE Transactions on Intelligent Transportation Systems*, vol. 23, no. 10, pp. 18951–18961, 2022.

[27] X. Shao, J. Zhang, L. Xu, and W. Zhang, "Appointed-time guaranteed adaptive fault-tolerant attitude tracking for quadrotors with aperiodic data updating," *Aerospace Science and Technology*, Article ID 107881, 2022.

[28] W. Zhang, X. Shao, W. Zhang, J. Qi, and H. Li, "Unknown input observer-based appointed-time funnel control for quadrotors," *Aerospace Science and Technology*, vol. 126, pp. 1–11, Article ID 107351, 2022.

[29] Q. Hou, S. Ding, and X. Yu, "Composite super-twisting sliding mode control design for PMSM speed regulation problem based on a novel disturbance observer," *IEEE Transactions on Energy Conversion*, vol. 36, no. 4, pp. 2591–2599, 2021.

[30] M. Yang, X. Lang, J. Long, and D. Xu, "Flux immunity robust predictive current control with incremental model and extended state observer for PMSM drive," *IEEE Transactions on Power Electronics*, vol. 32, no. 12, pp. 9267–9279, 2017.

[31] Y. Wang, H. T. Yu, N. J. Feng, and Y. C. Wang, "Non-cascade backstepping sliding mode control with three-order extended state observer for PMSM drive," *IET Power Electronics*, vol. 13, no. 2, pp. 307–316, Feb. 2020.

[32] J. Yang, S. H. Li, J. Y. Su, and X. H. Yu, "Continuous non-singular terminal sliding mode control for systems with mismatched disturbances," *Automatica*, vol. 49, no. 7, pp. 2287–2291, 2013.

[33] S. Yu, X. Yu, B. Shirinzadeh, and Z. Man, "Continuous finite-time control for robotic manipulators with terminal sliding mode," *Automatica*, vol. 41, no. 11, pp. 1957–1964, 2005.

[34] L. Yang and J. Y. Yang, "Nonsingular fast terminal sliding-mode control for nonlinear dynamical systems," *International Journal of Robust and Nonlinear Control*, vol. 21, no. 16, pp. 1865–1879, 2010.

[35] V. Srikanth and A. A. Dutt, "A comparative study on the effect of switching functions in SMO for PMSM drives," in *Proceedings of the 2012 IEEE Int. Conf. Power Electron., Drives and Energy Syst. (PEDES)*, pp. 1–6, Bengaluru, India, December 2012.

[36] S. F. Xiong, W. H. Wang, X. D. Liu, Z. Q. Chen, and S. Wang, "A novel extended state observer," *ISA Transactions*, vol. 58, pp. 309–317, Sep. 2015.

[37] S. Li and Y. P. Tian, "Finite-time stability of cascaded time-varying systems," *International Journal of Control*, vol. 80, no. 4, pp. 646–657, Feb. 2007.

[38] N. Boizot, E. Busvelle, and J.-P. Gauthier, "An adaptive high-gain observer for nonlinear systems," *Automatica*, vol. 46, no. 9, pp. 1483–1488, 2010.